Supplement of Solid Earth, 17, 35–53, 2026
https://doi.org/10.5194/se-17-35-2026-supplement

Solid Earth Open Access EGU

Supplement of

Polyphase tectonic, thermal and burial history of the Vocontian basin revealed by U–Pb calcite dating

Louise Boschetti et al.

Correspondence to: Louise Boschetti (louise.boschetti@univ-tlse3.fr)

Content of this file

1- U-Pb image geochronology
2- Table S1: Analytical conditions
3- Table S2: Isotopic map characteristics (successfully dated unknowns)
4- Figure S1: Tomographic map of the Vocontian Basin

Introduction

These files first contain the analytical method of U-Pb image geochronology used in this study. Then there is Table 1, which shows the analytical conditions; Table 2, which shows the isopic map characteristics for the dated samples; and a figure, which shows the tomographic map that was used once during the discussion.

S1- U-Pb image geochronology

U-Pb geochronology via the in-situ Laser Ablation Inductively Coupled Mass Spectrometer (LA-ICP-MS) method was conducted at the Institut des Sciences Analytiques et de Physico-Chimie pour l'Environnement et les Matériaux (IPREM) laboratory (Pau, France). The sample (polished chip) was analysed with a femtosecond laser ablation system (Lambda3, Nexeya, Bordeaux, France), coupled to a sector-field ICP-MS Element XR (ThermoFisher Scientific, Bremen, Germany) fitted with the Jet Interface (Table S1), in June 2023. The aerosol produced by the ablation was carried to the ICP-MS by a tube (1/16" internal diameter) using a Helium stream (600 mL min^{-1}). Measured wash out time of the ablation cell was ~500-600 ms for helium gas considering the 99% criterion. To improve sensitivity, 10 mL min^{-1} of nitrogen was added to the twister spray chamber of the ICP-MS via a tangential inlet while helium flow was introduced via another tangential inlet located at the very top of the spray chamber. Measurements were performed under dry plasma conditions. The fs-LA-ICP-MS coupling was tuned on a daily basis in order to achieve the best compromise in terms of sensitivity, accuracy, particles atomization efficiency and stability. The additional Ar carrier gas flow rate, torch position and power were adjusted so that the U/Th ratio was close to 1 +/-

0.05 when ablating the NIST SRM612 glass. Detector cross-calibration and mass bias calibration were checked daily using the appropriate sequence of the Element Software.

The femtosecond laser operates at an UV wavelength of 257 nm and delivers 360 fs pulses. The laser source was adjusted to operate at a repetition rate of 500 Hz with a fluence of ~2 µJ per pulse. Complex trajectories can be realized by moving the laser beam (15 µm diameter) across the surface of the sample using the rapid movement of galvanometric scanners combined with the high repetition rate.

A rapid screening of all samples (n = 50) was first realised to select the ones suitable for dating. It consists in monitoring the ^{238}U and ^{206}Pb masses at random locations without recording the signal, up to finding areas with $^{238}U/^{206}Pb$ ratios above 1. For the selected samples (n = 26), isotopic maps were built at the same location and used for in situ U-Pb dating following the method described in Hoareau et al. (in review). In detail, a blank was first acquired during the duration of a line scan (25 to 239 s). For mapping, lines of 25 µm height, separated by 25 µm so that they are adjacent to each other, were obtained using a back-and-forth movement of the laser (at 5 mm s^{-1}) combined with a stage movement rate of 25 µm s^{-1}. They correspond to 25 to 239 s of analysis per linear scan, followed by a 25 s break for the analysed unknown sample. The total analysis time for 7 to 35 linear scans was of ~21 to ~61 min for the maps of a surface of ~0.46 to ~1.84 mm^2 (see Table S2 for successful samples). The ablation depth was about 40 µm as measured with a digital microscope Keyence VH-7000. Before analysis, all samples were pre-cleaned with the laser using a stage movement rate of 200 µm s^{-1}.

The ^{238}U, ^{232}Th, ^{208}Pb, ^{207}Pb, and ^{206}Pb masses were selected, reaching a total mass sweep time of about ~78 ms (2024) or ~55 ms (2025). The limits of detection for ^{206}Pb and ^{238}U were ~0.14 and ~0.025 ppb in 2024, and ~0.18 and ~0.011 ppb in 2025, respectively, as calculated by Iolite 4 using the equation of Howell et al. (2010).

U-Pb data were processed using Iolite 4 software (Paton et al., 2011) and the VizualAge_UcomPbine Data Reduction Scheme for background correction and normalization (Chew et al. 2014). After line selection and background correction, NIST SRM614 glass was used as the primary reference material for normalization (mass drift and interelement fractionation) of both Pb/Pb and Pb/U isotope data. Correction of additional matrix-related offset of the $^{206}Pb/^{238}U$ ratio used WC-1 calcite reference material (age 254.4 ± 6.4 Ma), using the method of Roberts et al. (2017). To that end, small maps of the primary RMs (~0.1 mm^2, analysis time of ~3.5 min) were produced before and after each analysis of unknown samples (standard bracketing), under conditions like those described above, and corrections calculated from linear interpolations between the analyses. The Duff Brown Tank limestone (Age 64.04 ± 0.67; Hill et al., 2016) and AUG-B6, a tectonic calcite vein from the Paris basin (France) dated by U–Pb LA-ICP-MS at about 42 to 43 Ma in several laboratories (Pagel et al., 2018; Blaise et al., 2023), were used as validation reference material. From the 26 samples selected for dating, 18 proved successful. For 9 of these, due to low ^{238}U, ^{206}Pb and/or ^{207}Pb concentrations, the ~55/78 ms dwell times used proved too short, and a significant number of sweeps had zero counts on the monitored Pb masses. After background correction, this resulted in large positive or negative spikes in the calculated Pb/Pb and Pb/U ratios using a mean of ratios approach, resulting in biased age calculations (see Hoareau et al. (in review) for details). To avoid such spikes, all mass counts were averaged over 3 to 8 mass sweeps prior to treatment with Iolite, resulting in a final mass sweep value of ~220 to 440 ms (Table S2). For consistency across the different samples, this approach was also used for reference materials within a session (e.g., Picazo et al., 2019). A comparison between Pb/Pb and Pb/U ratios obtained for reference materials with and without this initial treatment showed no significant difference. No common lead correction nor downhole fractionation correction were made. The ratio values for each pixel are obtained in the “Imaging” section of Iolite. The software allows the operator to

filter out pixels that are considered anomalous or to select a specific area of the produced isotopic mass. Here, for the unknown samples, pixels with negative counts per second values of ^{238}U, ^{207}Pb and ^{206}Pb were excluded by default. Additional criteria include removal of pixels with $^{207}Pb/^{206}Pb$ ratios higher than 2 or 2.5 (1-2, 31a and AUG-B6 (10/02/2025)), and ^{238}U, ^{207}Pb and ^{206}Pb lower than 1000 cps (BON23-01). The resulting number of pixels used for successful age calculation ranges between 3670 and 33091.

An in-house Python script was then used as part of the Python API embedded in Iolite 4. This script as well as the ones described below are publicly available (Hoareau et al., in review). The Python script allows to reconstruct isotopic ratio matrices from pixel values, to add excess variance to individual ratio uncertainties, to correct of matrix-related offset of the $^{206}Pb/^{238}U$ ratio, to split the isotopic image maps into virtual spots forming a grid, and to calculate the mean and its uncertainty for each spot, for all ratios. First, for each virtual spot the mean of ratios is calculated, pixels identified as outliers, if any, are removed (i.e, pixel ratio values outside the 95% confidence interval of the standard error), and the mean recalculated. Second, excess variance calculated by Iolite 4 using all ablation lines of NIST 614 (typically 1.5-2.5% (2s) for $^{238}U/^{206}Pb$ and 0.1-0.3 (2s) for $^{207}Pb/^{206}Pb$) is added by quadrature to the uncertainties of each virtual spot obtained from the unknowns (and WC-1) within the session. For correction of the matrix-related offset, the isotopic maps of WC-1 produced in the analytical session (standard bracketing) are split in virtual spots of size like those used on the unknowns. The mean and uncertainty values of $^{238}U/^{206}Pb$ and $^{207}Pb/^{206}Pb$ ratios are then plotted in TW diagrams using IsoplotR (Vermeesch, 2018) to calculate the ages used for correction. After these first steps, virtual spots are calculated for the unknowns. Whereas their minimum height (vertical size) is limited to that a line (25 µm), their minimum width (horizontal size) can theoretically be as small as that of a few microns (few pixels). The script allows to change the grid location makes it possible to calculate several dozens of ages corresponding to each grid

location. This process allows to assess the homogeneity of the sample in terms of age by using weighted mean statistics, and to select the best age obtained in terms of precision and statistical robustness (MSWD value and p). Finally, virtual spots with high individual uncertainties can be filtered out. In the present study, for the unknown sample the virtual spots displaying uncertainty higher than 30% were removed (15% for BON23-02).

As a final step, ages were calculated with Tera-Wasserburg diagrams generated with an R script using the *age* and *concordia* functions of IsoplotR library. Systematic uncertainties were then added quadratically to the final age. They comprise the decay constant uncertainty of ^{238}U (0.1 %, 2 s), the $^{238}U/^{206}Pb$ ratio uncertainty of WC1, as estimated by Roberts et al. (2017) (2.7 %, 2 s), and the long-term excess variance taken as 2.0 % (2 s). Ages are quoted directly with the systematic uncertainties.

Table S1: Analytical conditions

Laboratory & Sample Preparation	
Laboratory name	Institut des sciences analytiques et de physico-chimie pour l'environnement et les matériaux (IPREM), UPPA, Pau (France)
Sample type/mineral	Calcite
Sample preparation	In situ in thick sections
Imaging	Yes
Laser ablation system	
Make, Model & type	Lambda 3, Nexeya (France)
Ablation cell	Home-made (home-designed) two volumes ablation cell. The large cell has a rectangular shape and a volume of 11.25 cm^3 (75 x 25 x 6 mm size) while the small one, placed above the sample is of 10 mm diameter.
Laser wavelength (nm)	257 nm
Pulse duration (fs)	360 fs
Fluence ($J.cm^{-2}$)	5-8 $J.cm^{-2}$
Repetition rate (Hz)	500 Hz
Gas blank (s)	25 to 239 s per image (1 line)
Ablation duration (s)	25 to 239 s per line

Washout and/or travel time in between analyses (s)	Wash out time ~500-600 ms. 25 s of break between lines to allow data processing.
Spot diameter (µm)	15 µm
Sampling mode / pattern	Ablation lines (25 µm-height) made by combining laser beam movement across the surface (5 mm/s) and stage movement (25 µm/s). 25 µm between lines.
Cell Carrier gas (L/min)	He = 0.600 L/min
ICP-MS Instrument	
Make, Model & type	ICPMS Thermo Fisher ElementXR HR Jet Interface
RF power (W)	1000 - 1100W
Cooling gas flow rate	16 L min^{-1}
Auxiliary gas flow rate	1 L min^{-1}
Nebuliser gas flow rate	0.5 L min^{-1}
Masses measured	206, 207, 208, 232, 238
Samples per peak	30
Mass window	10 %
Sample time	3 ms
Settling time	1 ms
Mass sweep	78 ms (2024) or 55 ms (2025)
Averaged mass sweep	Depends on samples (made during data processing) – by default no
Resolution	300
Sensitivity	Percentage of ions detected with regard to atoms ablated is ~0.04% for U, as calculated with NIST SRM 614
Data Processing	
Calibration strategy	Calibration by standard bracketing; NIST SRM 614 for Pb-Pb and WC-1 calcite for Pb-U
Reference Material info	Primary: NIST SRM 614 - Woodhead and Hergt (2001) WC1: 254.4 ± 6.4 Ma (2s) - Roberts et al., 2017 Secondary: Duff Brown 64.04 ± 0.67 Ma (2s) - Hill et al., 2016 AUG-B6: ~42-43 Ma - Pagel et al., 2018; Blaise et al., 2023
Data processing package used / Correction for LIEF	Element XR acquisition software, data processing with Iolite 4 and in-house Python/R code. Age determination through virtual spot discretization.
Common-Pb correction, composition and uncertainty	No common Pb correction. Excess uncertainty calculated by Iolite (Paton et al., 2011) based on NIST SRM 614 are added to individual uncertainties. Ages in the figures are quoted at 95% absolute uncertainties and include systematic uncertainties (WC1 2.7%, decay constants 0.1%, long-term uncertainty 2%), propagation is by quadratic addition.
Quality control / Validation	5 analyses of Duff Brown gave 63.45 ± 2.8 Ma, 69.2 ± 2.6 Ma (anchored to common Pb value of 0.738), 62.9 ± 2.2 Ma (anchored), 63.0 ± 3.3 Ma and 63.3 ± 3.2 Ma. analyses of AUG-B6 gave 42.7 ± 2.1 Ma, 39.8 ± 1.6 Ma, 43.2 ± 2.0 Ma, 45.2 ± 1.7 Ma and 44.5 ± 2.0 Ma.

117

118

119

120

Table S2: Isotopic map characteristics (successfully dated unknowns)

Sample	Line scan duration (s)	Number of line scans	Duration of mapping (min)	Map dimensions (mm x mm)	Map area (mm^2)	Mass sweep duration (ms)	Number of pixels (before filtering)	Number of pixels (after filtering)
1-1	127.3	15	38.1	3.18 x 0.375	1.19	78	24315	24237
1-2	79.6	18	31.4	1.99 x 0.450	0.896	78	18252	17797
9a2	54.5	24	31.8	0.925 x 0.500	0.818	234	5550	5436
9b1	45	26	30.3	1.36 x 0.600	0.731	234	4966	4966
11a	99.5	27	56.0	1.12 x 0.650	1.68	78	13581	13581
12a	98	30	61.5	2.49 x 0.675	1.84	234	12480	12460
12b	55.2	24	32.1	2.45 x 0.750	0.828	234	5850	5788
13b	82.9	31	55.7	1.38 x 0.600	1.61	78	32736	32736
14a	44.8	35	40.7	2.07 x 0.775	0.980	78	19985	19978
14b	33.8	29	28.4	1.12 x 0.875	0.613	234	4176	4052
14b-2	36.1	21	21.4	0.845 x 0.725	0.474	78	9660	9651
16d	42.8	23	26.0	0.902 x 0.525	0.615	78	12535	12535
19b	59.2	25	35.1	1.48 x 0.625	0.925	220	6725	6666
22c	79.3	23	40.à	1.98 x 0.575	1.14	55	33097	33091
28b	59.5	33	46.5	1.49 x 0.825	0.616	55	17888	17867
31a	239.4	7	30.8	5.98 x 0.175	1.05	55	30422	29927
BON23-01	95	21	42.0	2.37 x 0.525	1.25	55	36204	27023
BON23-02	58.8	30	41.9	1.47 x 0.750	1.10	220	8010	7984
BON23-03	179.6	9	30.7	4.49 x 0.225	1.01	440	3672	3670
GLAN23-02	36.9	31	32.0	0.922 x 0.775	0.715	220	5208	5208

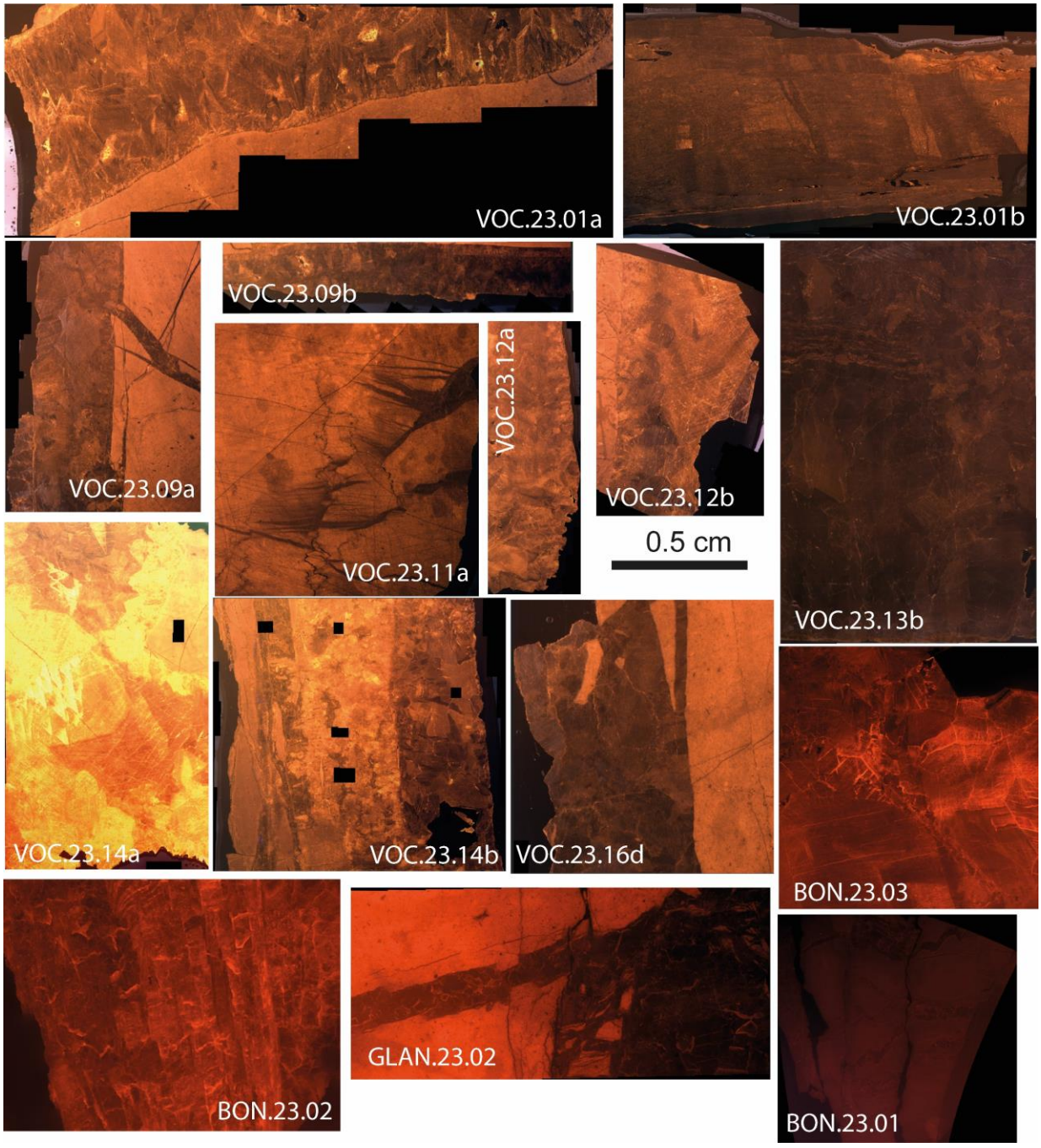

Figure S1: Cathodoluminescence for each dated sample.

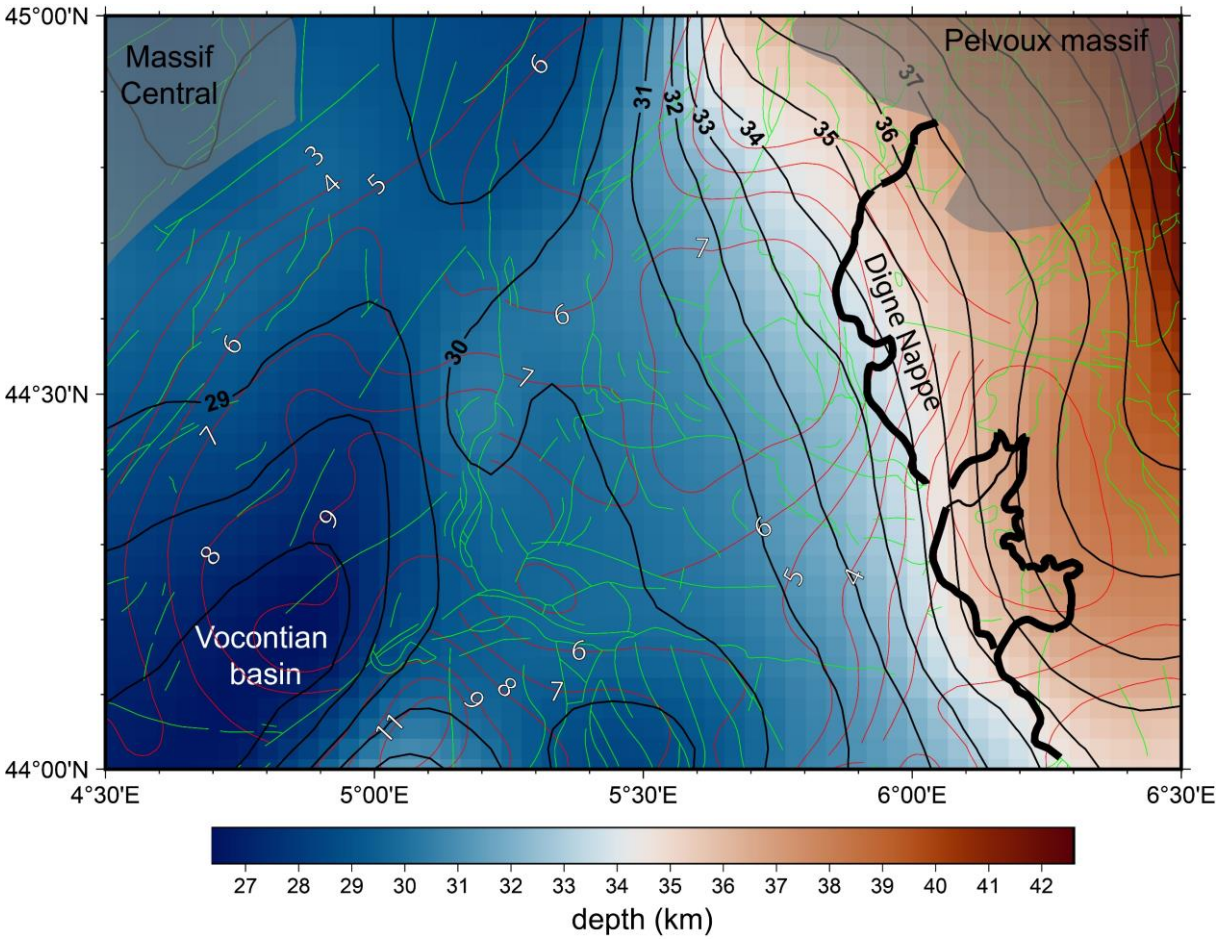

Figure S2: Crustal thickness and the region of the Vocontian Basin. Black line: Moho depth as inferred from Schwartz et al. (2024). Red: Thickness of the base the Trias. Green: Faults. Bold black line: Digne Nappe.

References

Blaise, T., Augier, R., Bosch, D., Bruguier, O., Cogne, N., Deschamps, P., Guihou, A., Haurine, F., Hoareau, G., Nouet, J.: Characterisation and interlaboratory comparison of a new calcite reference material for U-Pb geochronology - The “AUG-B6” calcite-cemented hydraulic breccia. 2023 Goldschmidt Conference, 9-14 July, Lyon, France, 2023.

Chew, D. M., Petrus, J. A., Kamber, B. S.: U–Pb LA–ICPMS dating using accessory mineral standards with variable common Pb. Chem. Geol., 363, 185-199, 2014

Hill, C. A., Polyak, V. J., Asmerom, Y., Provencio, P.: Constraints on a Late Cretaceous uplift, denudation, and incision of the Grand Canyon region, southwestern Colorado Plateau, USA, from U-Pb dating of lacustrine limestone. Tectonics, 35, 896-906, 2014

Hoareau, G., Claverie, F., Pecheyran, C., Barbotin, G., Perk, M., Beaudoin, N., Lacroix, B., Rasbury, T.: The virtual spot approach: a simple method for image U-Pb carbonate geochronology by high-repetition rate LA-ICP-MS. EGUsphere [preprint], https://doi.org/10.5194/egusphere-2024-2366, in review

Howell, D., Griffin, W.L., Pearson, N.J., Powell, W., Wieland, P., O’Reilly, S.Y.: Trace element partitioning in mixed-habit diamonds, Chem. Geol., 355, 134-143, 2013.

Pagel, M., Bonifacie, M., Schneider, D., Gautheron, C., Brigaud, B., Calmels, D., and Chaduteau, C., 2018. Improving paleohydrological and diagenetic reconstructions in calcite veins and breccia of a sedimentary basin by combining Δ47 temperature, δ^{18}Owater and U-Pb age, Chem. Geol., 481, 1-17. https://doi.org/10.1016/j.chemgeo.2017.12.026, 2018, 2018.

Paton, C., Hellstrom, J., Paul, B., Woodhead, J., Hergt, J.: Iolite: Freeware for the

visualisation and processing of mass spectrometric data. Journal of Analytical Atomic Spectrometry, 26, 2508, doi:10.1039/c1ja10172b, 2011.

Picazo, S.M., Ewing, T.A., Müntener, O, 2019. Paleocene metamorphism along the Pennine–Austroalpine suture constrained by U–Pb dating of titanite and rutile (Malenco, Alps). Swiss J Geosci 112, 517–542., 2019.

Roberts, N.M., Rasbury, E.T., Parrish, R.R., Smith, C.J., Horstwood, M.S., Condon, D.J.: A calcite reference material for LA-ICP-MS U-Pb geochronology. Geochem., Geophys., Geosyst., 18, 2807-2814, 2017.

Schwartz, S., Rolland, Y., Nouibat, A., Boschetti, L., Bienveignant, D., Dumont, T., ... & Mouthereau, F.: Role of mantle indentation in collisional deformation evidenced by deep geophysical imaging of Western Alps. Communications Earth & Environment, 5(1), 17. https://doi.org/10.1038/s43247-023-01180-y, 2024.

Vermeesch, P.: IsoplotR: A free and open toolbox for geochronology. Geosci. Front., 9, 1479-1493, 2018.

Woodhead, J.D., Hergt, J.M.: Strontium, neodymium and lead isotope analyses of NIST glass certified reference materials: SRM 610, 612, 614. Geostand. Newslett., 25, 261-266, 2001.